

82N 32407

RTI/1796/00-04F

NASA CR-165970

CONCEPTS FOR ON-BOARD SATELLITE IMAGE REGISTRATION

FINAL REPORT

VOLUME FOUR

IMPACT OF DATA SET SELECTION ON SATELLITE ON-BOARD SIGNAL PROCESSING

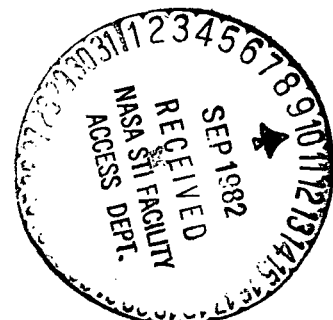
Prepared Under Contract NAS1-15768

Prepared for



NATIONAL AERONAUTICS AND SPACE ADMINISTRATION  
Langley Research Center  
Hampton, Virginia 23665

September 1982



CONCEPTS FOR ON-BOARD SATELLITE IMAGE REGISTRATION

Final Report

Volume Four

IMPACT OF DATA SET SELECTION ON SATELLITE ON-BOARD SIGNAL PROCESSING

Prepared Under Contract NAS1-15768

by

W. H. Ruedger, J. V. Aanstoos

Research Triangle Institute  
Research Triangle Park, North Carolina 27709

and

W. E. Snyder

North Carolina State University  
Raleigh, North Carolina 27650

Prepared for



NATIONAL AERONAUTICS AND SPACE ADMINISTRATION  
Langley Research Center  
Hampton, Virginia 23665

September 1982

## PREFACE

This report was prepared by the Research Triangle Institute, Research Triangle Park, North Carolina, under Contract NAS1-15768. The work has been administered by the Electronics Devices Research Branch of the Flight Electronics Division, Langley Research Center, National Aeronautics and Space Administration. Mr. Marvin E. Beatty, III served as Technical Representative.

These studies began on January 16, 1981 and were completed on July 15, 1982. Mr. W. H. Ruedger served as Project Leader. Mr. J. V. Aanstoos completed the project team. Dr. W. E. Snyder, North Carolina State University, served as Consultant to the programs.

## TABLE OF CONTENTS

	<u>Page</u>
PREFACE. . . . .	iii
LIST OF ILLUSTRATIONS. . . . .	v
LIST OF TABLES . . . . .	vi
1.0 INTRODUCTION. . . . .	1
2.0 DATA SET SELECTION - FILE . . . . .	2
3.0 CLOUD COVER STATISTICS. . . . .	5
4.0 DATA COMPRESSION. . . . .	8
4.1 Introduction . . . . .	8
4.2 Pulse Code Modulation (PCM). . . . .	8
4.3 Predictive Techniques. . . . .	11
4.4 Differential Pulse Code Modulation (DPCM). . . . .	11
4.5 Two Dimensional DPCM . . . . .	13
4.6 DPCM With Multispectral Predictor. . . . .	17
5.0 DYNAMIC COMPANDING. . . . .	20
6.0 ADDITIONAL TECHNIQUES FOR DATA RATE REDUCTION . . . . .	32
7.0 PACKETIZATION . . . . .	33
8.0 RECOMMENDATIONS . . . . .	34
REFERENCES . . . . .	35

# LIST OF ILLUSTRATIONS

<u>Figure No.</u>	<u>Title</u>	<u>Page</u>
2-1	Target spectral radiance signatures. . . . .	3
2-2	99% confidence polygons, sun 41 to 60° from zenith . . . .	4
3-1	Cloud cover distributions demonstrating regional homogeneity for Region 1 . . . . .	6
4-1	PCM Encoding: (a) components of a PCM encoder, (b) Four- bit binary representation of amplitude levels between 0 to 15. . . . .	9
4-2	DPCM components. . . . .	12
4-3	Two-dimensional DPCM . . . . .	15
4-4	SNR versus rate of DPCM of two-dimensional, separable covariance causal model images and its comparison with line-by-line DPCM and with PCM. . . . .	16
4-5	DPCM for multispectral data. . . . .	19
5-1	MSS (band 6) from Landsat 2/North Carolina coastal waters (areas of analysis are shown in rectangular areas) . . . . .	21
5-2	Analysis area no. 1, rural terrain . . . . .	22
5-3	Histogram of first analysis area, band 4 . . . . .	23
5-4	Histogram of first analysis area, band 5 . . . . .	24
5-5	Histogram of first analysis area, band 6 . . . . .	25
5-6	Histogram of first analysis area, band 7 . . . . .	26
5-7	Analysis area no. 2, land/water contrast . . . . .	27
5-8	Histogram of analysis area no. 2, band 4 . . . . .	28
5-9	Histogram of analysis area no. 2, band 5 . . . . .	29
5-10	Histogram of analysis area no. 2, band 6 . . . . .	30
5-11	Histogram of analysis area no. 2, band 7 . . . . .	31

## LIST OF TABLES

<u>Table No.</u>	<u>Title</u>	<u>Page</u>
4-1	Image transmission coding techniques . . . . .	10

## 1.0 INTRODUCTION

NASA has embarked on a program to increase the effectiveness and efficiency of the system that couples the user of space data with the sensors that acquire this data. This program, the NASA End-to-End Data System (NEEDS), addresses the identification, development, and demonstration of data handling techniques and technologies which are required to accomplish these goals.

More specifically, the NEEDS program goals present a requirement for on-board signal processing to achieve user-compatible, information-adaptive data acquisition. These signal processing functions comprise a major constituent of the Information Adaptive System (IAS), a significant module of the NEEDS concept. The IAS essentially consists of the spaceborne portion of NEEDS exclusive of telemetry, support, and housekeeping functions.

This volume addresses the impact of data set selection on data formatting required for efficient telemetering of the acquired sensor data. More specifically, the FILE algorithm developed by Martin-Marietta[1] provides a means for the determination of those pixels for which the earth's surface is obscured by clouds. Subsequent deletion of these pixels from the data stream effects an improvement in the achievable system throughput. This is necessary in that future sensors requiring throughput of 370 Mb/sec (i.e., the MLA aboard the OEOS) will use the TDRSS as their telemetry vehicle with a capacity of only 120 Mb/sec.

It will be seen that based on the lack of statistical stationarity in cloud cover, spatial distribution periods exist where data acquisition rates exceed the throughput capacity. The study therefore addresses various approaches to data compression and truncation as applicable to this sensor mission. Two new and novel approaches will be posed: that of band-to-band DPCM and that of dynamic companding. The volume concludes with a recommendation for further study.

## 2.0 DATA SET SELECTION - FILE[1]

The data set selection algorithm addressed by this study is the Feature Identification and Location Experiment (FILE) being developed for NASA (LaRC) under contract by Martin-Marietta. The goal of this program is to test a technique using spectral-radiance ratio detection autonomously for classifying picture elements in a solid-state camera image of the earth. Initially in the program, pixel classification focused on four main groups: vegetation, bare land, water, and clouds or snow/ice. Previous studies had shown that these four categories can be identified by radiance measurements at two discrete wavelengths: 0.65 and 0.85  $\mu\text{m}$ . Figure 2-1 shows how the various categories can be separated by radiance ratioing at these two wavelengths. Water and vegetation can be separated from clouds, snow (ice), and bare land on the basis of the IR/red ratio alone. Bare land can be separated from clouds and snow on the basis of overall radiance level with approximate knowledge of solar illumination angle. Figure 2-2 shows how the voltages from the imaging camera are used to provide this feature classification. The 99 percent confidence polygons are based on a computer model considering such parameters as visibility, illumination angle, sensor noise, pixel uniformity and dark current, viewing angle, variations in bare land and vegetation types, and some variation in water turbidity.

More recent efforts by Martin-Marietta have addressed a cloud detector capable of discriminating between clouds and snow/ice. It is known that both clouds and snow/ice have a high reflectance in the visible spectrum. However, at 1.55  $\mu\text{m}$  only clouds maintain a high reflectance. The addition of this band forms the basic ingredient of the "FILE II" algorithm to which the present study is addressed.



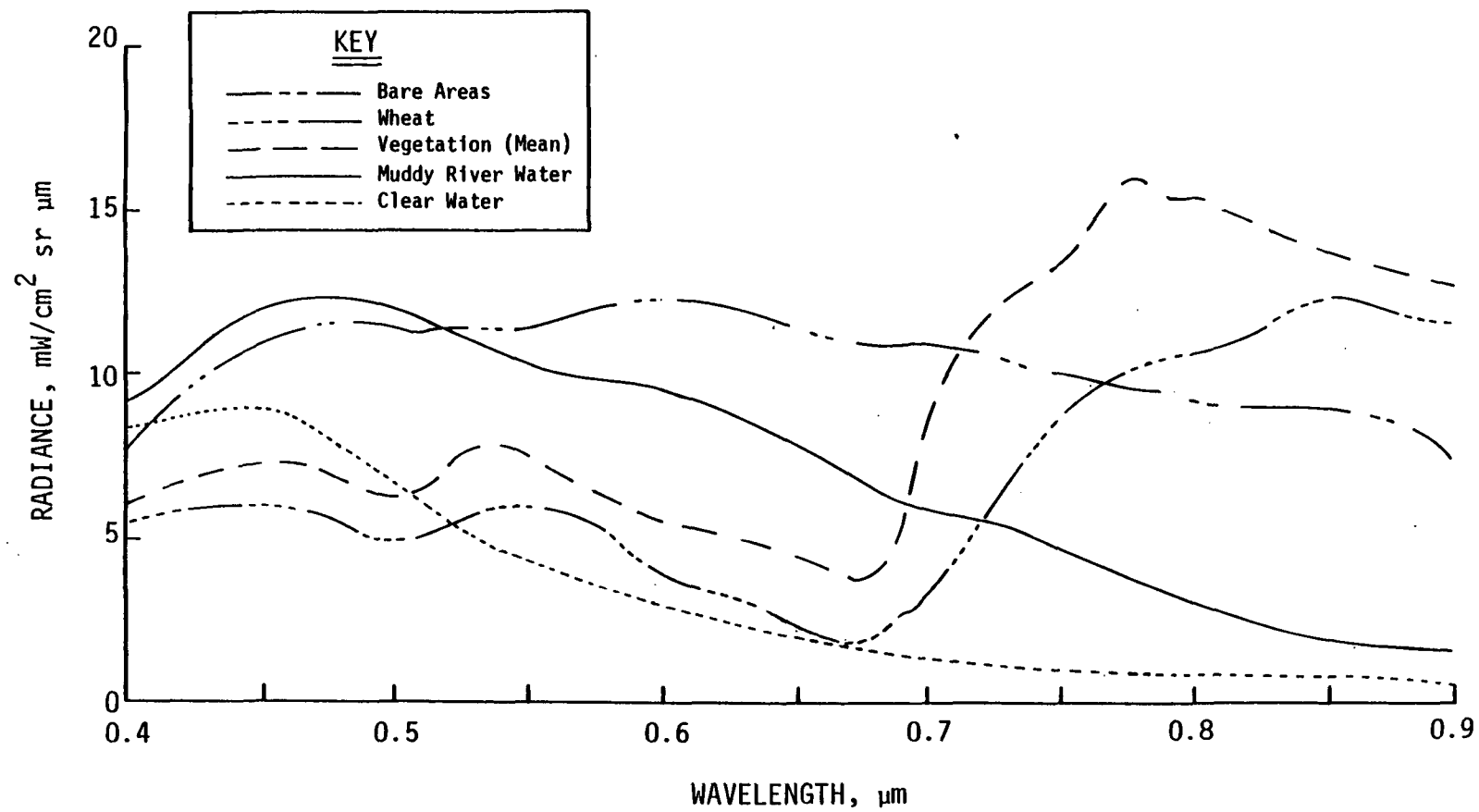


Figure 2-1. Target spectral radiance signatures. [1]

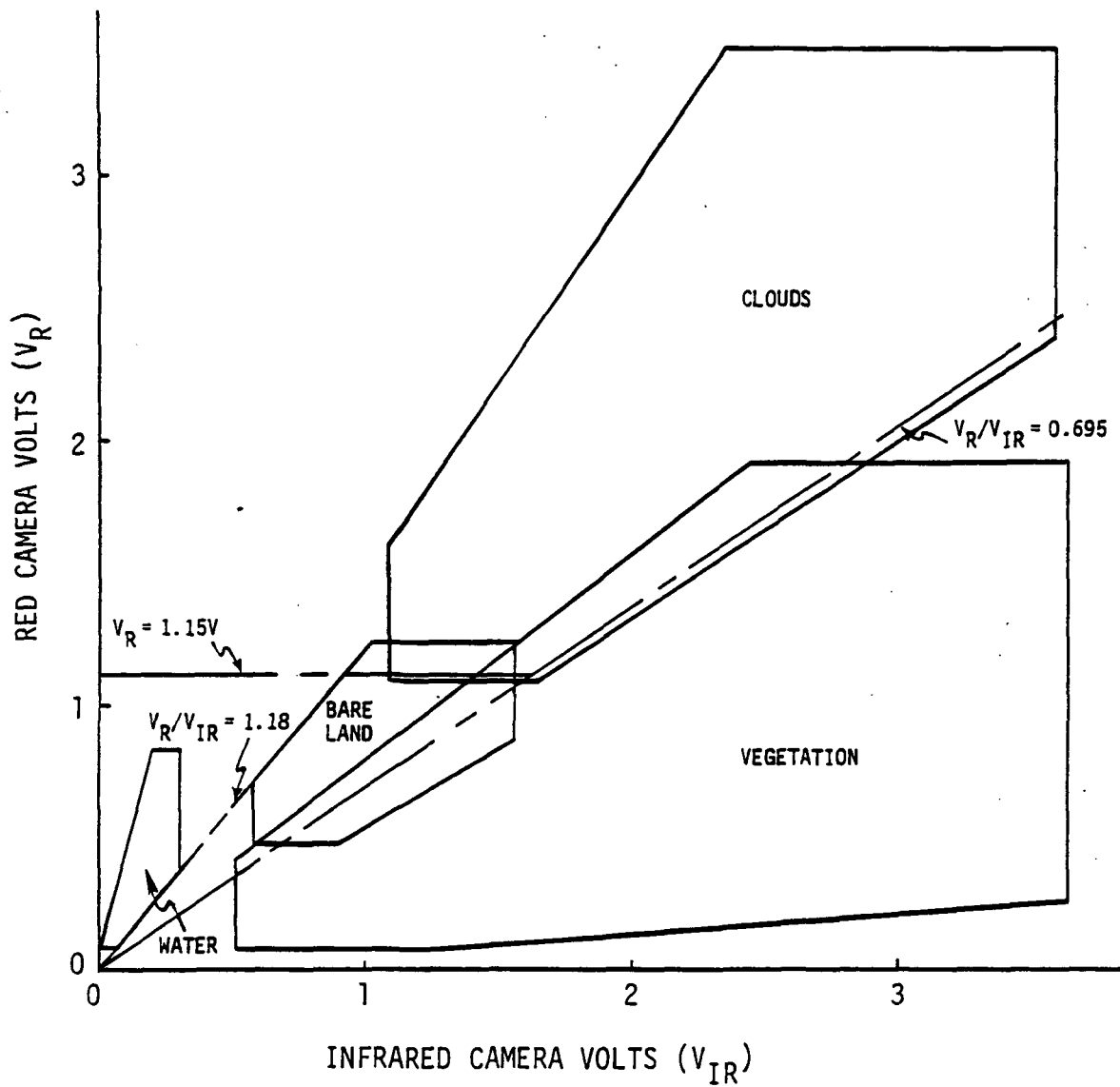


Figure 2-2. 99% confidence polygons, sun 41 to 60° from zenith. [1]

### 3.0 CLOUD COVER STATISTICS

To take advantage of the FILE algorithm's ability to determine cloud pixels, the data in cloud-free regions must be buffered until cloud pixels occur. At that time the buffer is dumped into the data stream and effectively compression occurs. In order to assess the size of an on-board memory to buffer the cloud-free data until cloud cover is encountered, it became necessary to examine the homogeneity of global cloud cover.

Various research studies indicate the global cloud cover to stay reasonably constant at about 40%[2]. If this were to demonstrate statistical stationarity, then bandwidth compression based on the editing of cloud pixels would be a highly feasible technique. There are, however, reports of large areas of the earth's surface with virtually no cloud cover. For example, Figure 3-1[3] presents frequency of cloud cover over three sample areas. Observe that during winter (1800 LST) 80% sky cover exists only 5% of the time, and less than 30% sky cover exists 70% of the time. From this type of data one could derive local estimates of the probability of cloud detection. However, this probability is not the appropriate statistic for buffer memory size determination. The required statistic is the distribution of distance between cloud pixels. Such data are likely to be Poisson distributed along-scan and behave in a Markov fashion from scan-to-scan. Numerous studies, in addition to the above references, have studied such cloud characteristics such as "viewability" of a region and the required number of looks to be certain of obtaining coverage. However, none were discovered which specifically addressed the statistics of distance-between-cloud-pixels. The data cannot easily be generated from image data in that extensive correlation with ground truth cloud identified pixels is required (also, it is doubtful that this ground truth data is readily available). However, by examination of the tabular data in [3], one can conclude that, quite often, extremely large areas of interest are almost totally cloud-free. Obviously, a buffer to meet this worst-case need is not reasonable. It is suggested that a nominal size buffer memory

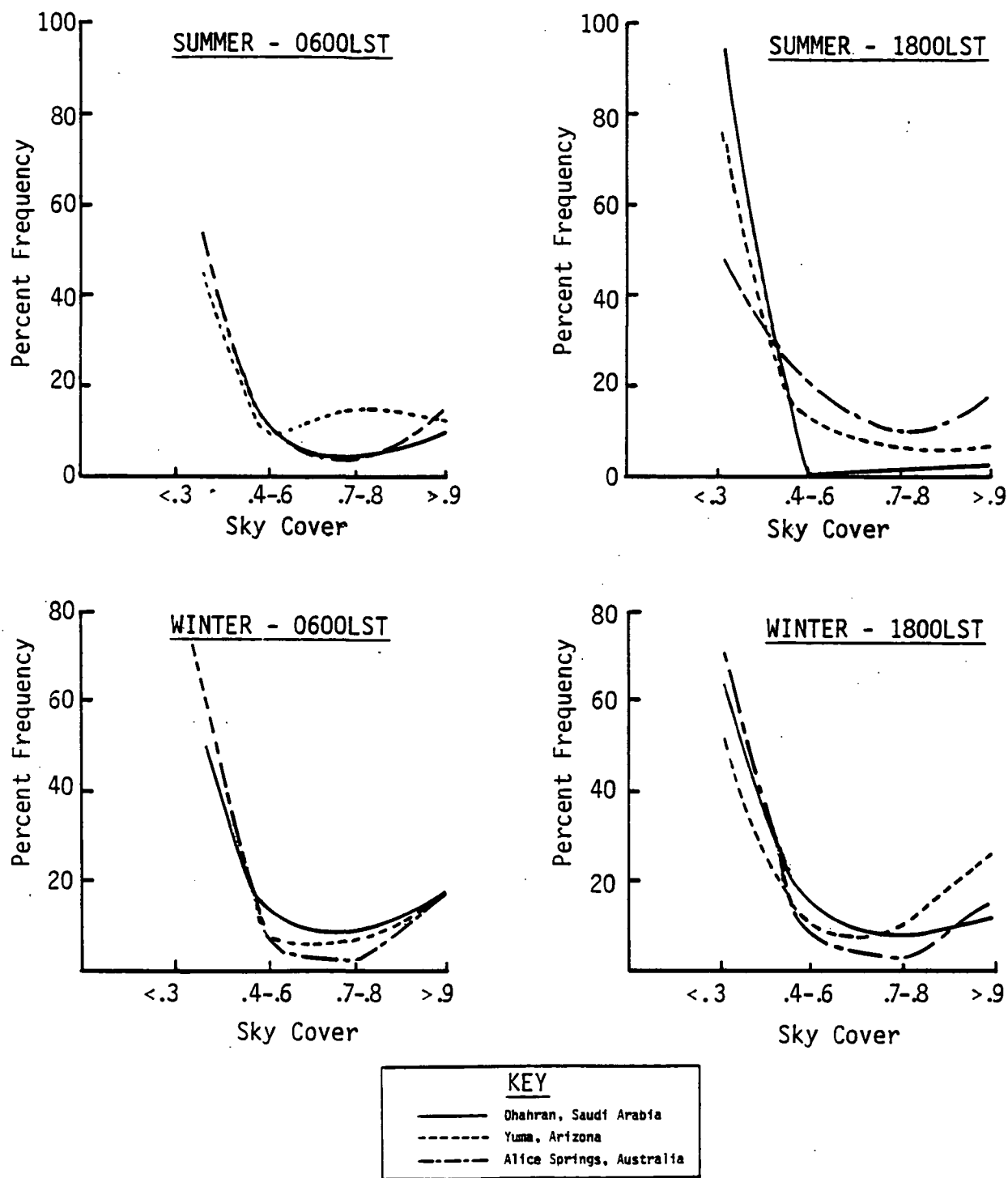


Figure 3-1. Cloud cover distributions demonstrating regional homogeneity for Region 1. [3]

be employed and that the data be further encoded or truncated to achieve compression. The combination of encoding and cloud cover elimination should work together very effectively, since those areas of the world which are low in cloud cover, e.g., deserts, also tend to be low in entropy. Novel approaches to achieve data compression are discussed in the following sections.

## 4.0 DATA COMPRESSION

### 4.1 Introduction

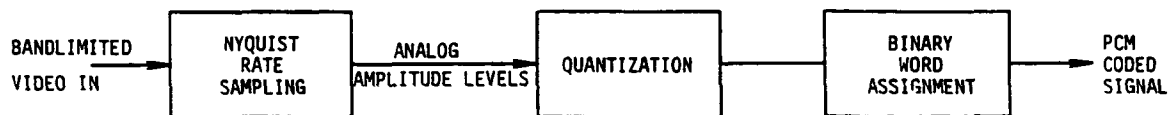
This section briefly presents well-known techniques of data compression as a setting for the introduction of what is considered to be a novel approach to compression: namely, band-to-band Differential Pulse Code Modulation. The theory of coding to achieve data compression is well documented in the literature ([4] and [5] are two excellent survey papers) and only the salient points will be addressed here.

Information coding may be divided into two general categories: namely information preserving and other codes which introduce distortions which are not usually obvious to the observer. The former removes statistical redundancy while the latter removes psycho-physical redundancy. Statistical redundancy removal results in compression ratios of usually less than a factor of two or three as exemplified by the Huffman and Shannon-Fano codes. Other information preserving codes of interest include Pulse Code Modulation (PCM) and predictive codes such as Differential PCM. As alluded to earlier these will be discussed in further detail in later paragraphs. Codes which remove psychophysical redundancy at the expense of some degree of distortion include transform codes such as Karhunen-Loeve, Hadamard, etc. These codes can achieve compression ratios on the order of several orders of magnitude in applications where only gross interpretation of pictorial data by a human observer is required.

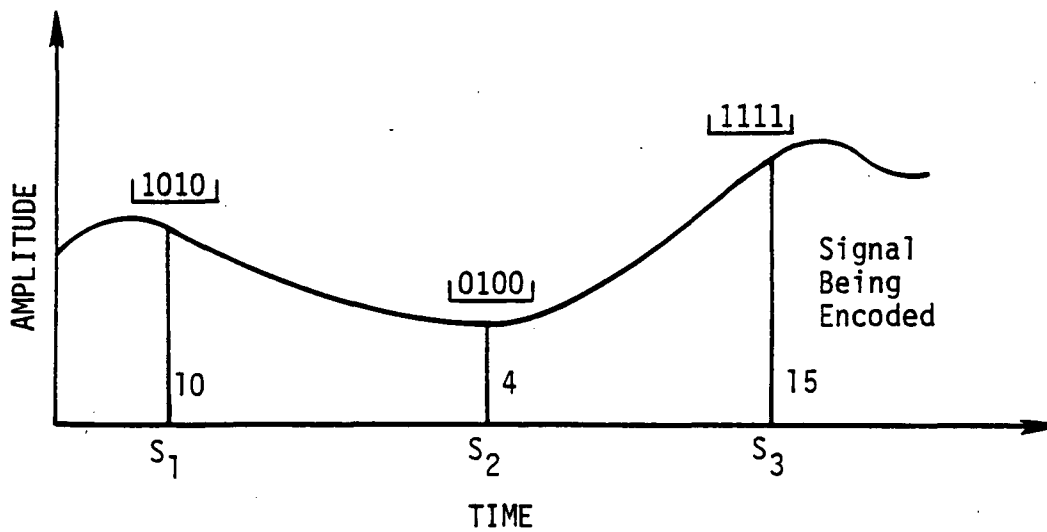
Table 4-1 indicates a "tree" diagram of coding techniques popularly used in image transmission.

### 4.2 Pulse Code Modulation (PCM)

PCM is a straightforward representation of a signal by a time discrete, amplitude discrete sequence of values. As shown in Figure 4-1 the waveform is sampled (usually at the Nyquist rate) and each sample quantized using some prespecified number of levels. A level is then represented by a binary word of length  $W$  such that the number of levels equals  $2^W$  (e.g.,



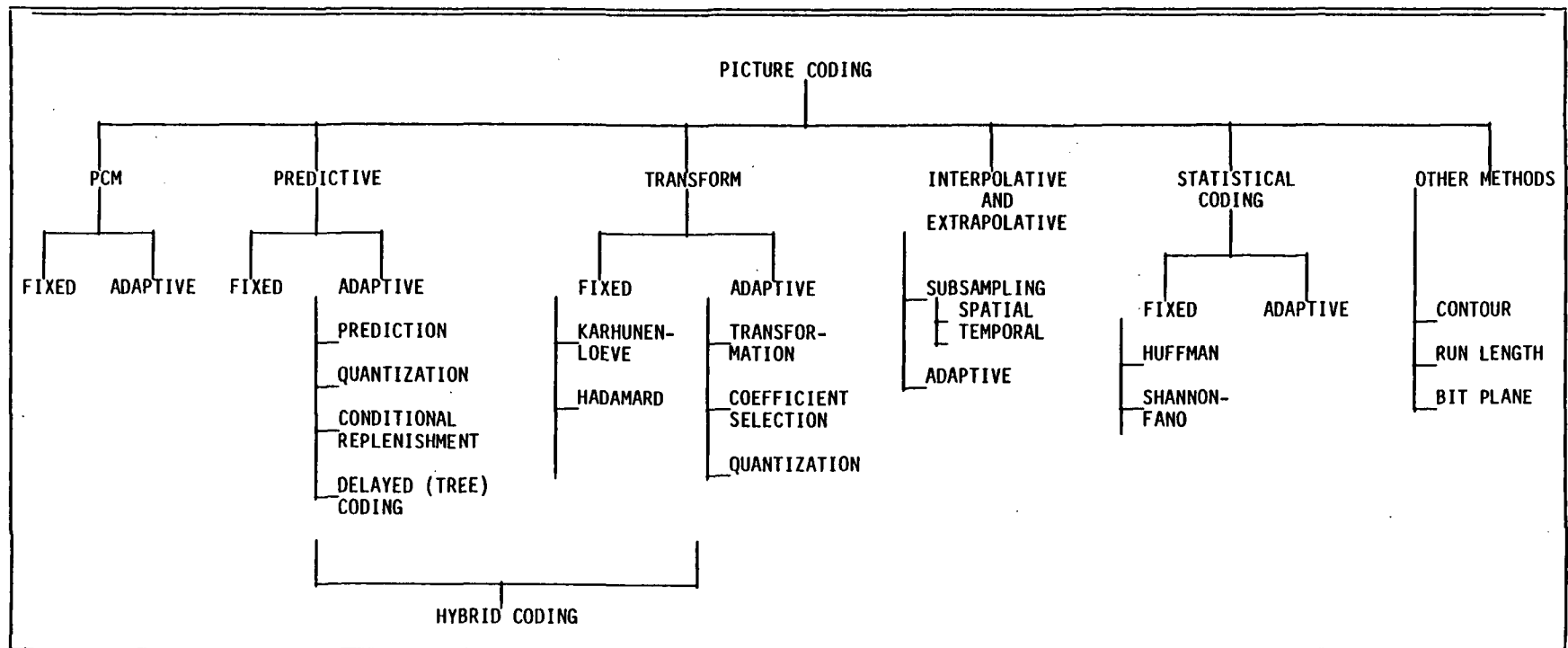
(a)



(b)

Figure 4-1. PCM Encoding: (a) components of a PCM encoder, (b) Four-bit binary representation of amplitude levels between 0 to 15. [4]

Table 4-1. Image transmission coding techniques.





an 8-bit word is used to represent 256 levels). PCM is not a redundancy removing code and is therefore often used as a baseline code for comparing other schemes.

### 4.3 Predictive Techniques[5]

Imagery in particular has both temporal and spatial redundancy from one sample to the next. As each sample is transmitted advantage can be taken of the fact that previously transmitted samples may contain information about it. Consider a sequence  $\{\mu_n\}$  and suppose the information in samples up to  $n=k-1$  has already been transmitted by some means. One can formulate a prediction of  $\mu_k$ ,  $\bar{\mu}_k^*$ , from these  $k-1$  samples and only transmit the difference sequence defined by

$$\epsilon_k \triangleq \mu_k - \bar{\mu}_k^*.$$

If  $\epsilon_k^*$  is the quantized value of  $\epsilon_k$ ,  $U_k^*$  the reproduced value of  $U_k$  is given by

$$\mu_k^* = \bar{\mu}_k^* + \epsilon_k^*.$$

### 4.4 Differential Pulse Code Modulation (DPCM)[5]

A widely used predictive technique for data transmission called DPCM is as shown in Figure 4-2. It is easy to deduce that the error in reproduction of  $U_k$  is given by

$$\delta_{\mu k} \triangleq \mu_k - \mu_k^* = \epsilon_k - \epsilon_k^* = q_k$$

and is equal to the error in quantization of  $\epsilon_k$ . To minimize the variance of the prediction error,  $\bar{\mu}_k^*$  should be the conditional mean

$$\bar{\mu}_k^* = E \left\{ \mu_k / \bar{U}_k^* \right\}$$

where  $\bar{U}_k^*$  is the set of past reproduced values, i.e.,

$$\bar{U}_k^* = \left\{ \mu_\ell^*, \ell < k \right\}.$$

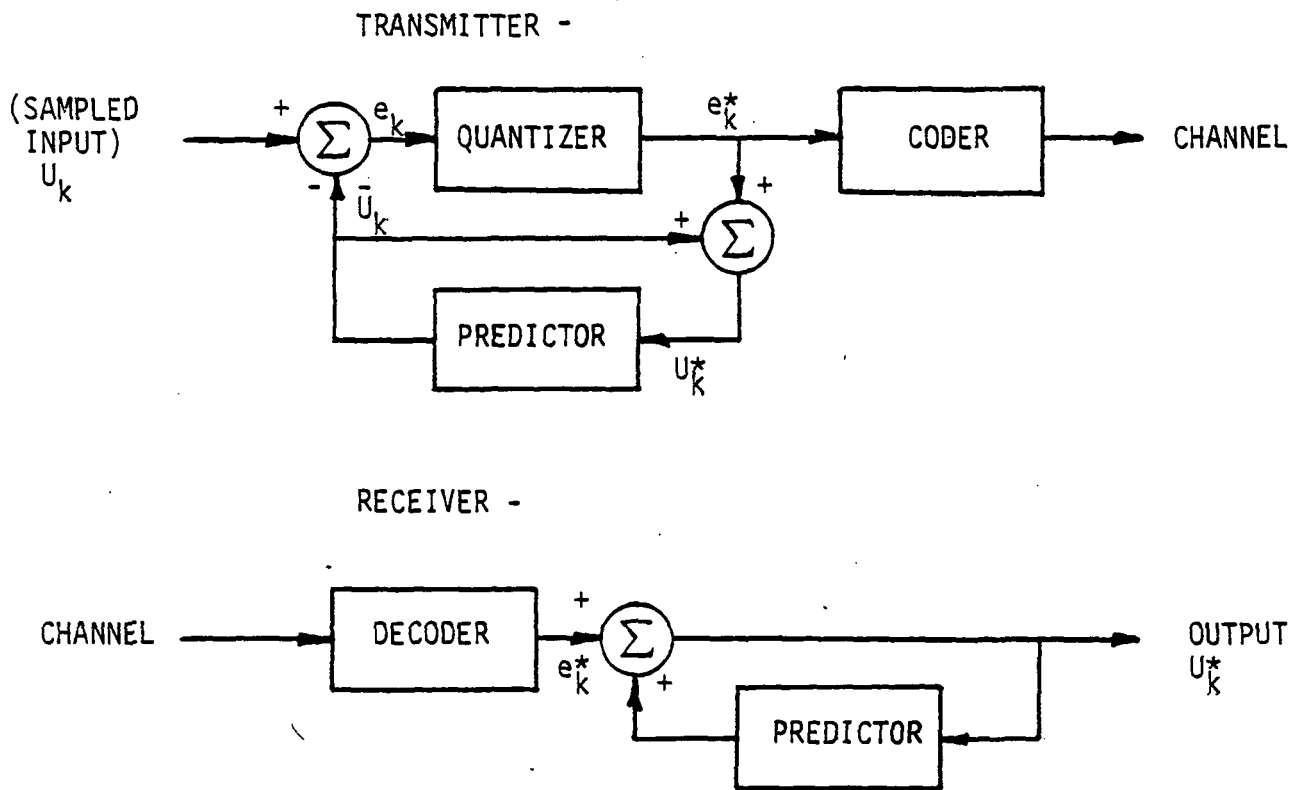


Figure 4-2. DPCM components.

The mean square distortion of  $\mu_k$  is given by

$$E[\delta_{\mu_k}^2] = \sigma_q^2(k)$$

and the minimum rate is

$$\eta_{DPCM} = 1/2 \log_2 \left( \frac{\sigma_e^2(k)}{\sigma_q^2(k)} \right)$$

where  $\sigma_e^2(k)$  is the prediction error variance. If conventional PCM were used, the minimum rate for  $\mu_k$  would be

$$\eta_{PCM} = 1/2 \log_2 \left( \frac{\sigma_u^2(k)}{\sigma_q^2(k)} \right)$$

for the same quantizing distortion  $\sigma_q^2(k)$ . The compression achievable,

$$\eta_{PCM} - \eta_{DPCM} = 1/2 \log_2 \left( \frac{\sigma_u^2(k)}{\sigma_e^2(k)} \right)$$

is seen to depend on the variance reduction by prediction (i.e., the ability to predict  $\mu_k$  and therefore on intersample dependence of the sequence  $\{\mu_k\}$ . If all the samples are independent then  $\bar{\mu}_k^* = E[\mu_k]$  and  $\sigma_u^2(k) = \sigma_e^2(k)$ , resulting in no advantage over PCM. The underlying philosophy of prediction quantization is to remove mutual redundancy between successive samples and quantize only the new information, i.e., the residuals. An important aspect of DPCM is that the prediction is based on the output rather than input samples from the past. As a result the predictor is in the feedback loop around the quantizer and quantizer noise is fed back to the quantizer input at the next step. This prevents accumulation of errors in the reconstructed signal  $\mu_k^*$ .

#### 4.5 Two Dimensional DPCM[5]

The above can be extended to two dimensions if a reasonable causal predictor for every pixel in the image is available. Consider, for example,

$$\mu_{i,j} = a_1 \mu_{i-1,j} + a_2 \mu_{i,j-1} - a_3 \mu_{i-1,j-1} + \epsilon_{i,j}$$

if  $a_3 = a_1 a_2$  and  $\epsilon_{ij}$  is a white noise field then this represents a random field with autocorrelation

$$r(m,n) = E\{\mu_{i,j} \mu_{i+m, j+n}\} = \sigma_\mu^2 a_1^{|m|} a_2^{|n|}.$$

The  $a_i$ ,  $i=1,2$  are the one step correlations of the field along the "i" and "j" axes. The prediction error variance is given by

$$\sigma^2 \triangleq E\{\epsilon_{i,j}^2\} = \sigma_\mu^2 (1-a_1^2)(1-a_2^2).$$

The DPCM equations corresponding to this model representations are:

Predictor:  $\bar{\mu}_{i,j}^* = a_1 \mu_{i-1,j}^* + a_2 \mu_{i,j-1}^* - a_3 \mu_{i-1,j-1}^*$

Quantizer Input:  $e_{i,j} = \mu_{i,j} - \bar{\mu}_{i,j}^*$

Reconstructor:  $\mu_{i,j}^* = \bar{\mu}_{i,j}^* + e_{i,j}^*$

The mechanization of the above is as shown in Figure 4-3.

For general imagery, the  $a_i$  are on the order of 0.95 from which it can be deduced[5] that two dimensional DPCM should require about 3.25 fewer bits/pel than PCM. Also, a three- or four-order predictor is usually sufficient and increasing the order above this does not provide any appreciable improvement in performance. The predictor coefficients are found by minimizing the mean-square prediction error of the input data and leads to a set of linear equations which can be solved with some notion of the image autocorrelation. The two-dimensional procedure differs from the one-dimensional case in that it can lead to an unstable causal model. This implies that the reconstruction filter can be unstable in the sense that transmission errors can be amplified at the receiver. The prediction model has to be stabilized by increasing either the prediction error or the order of the predictor before it is used in the DPCM algorithm.

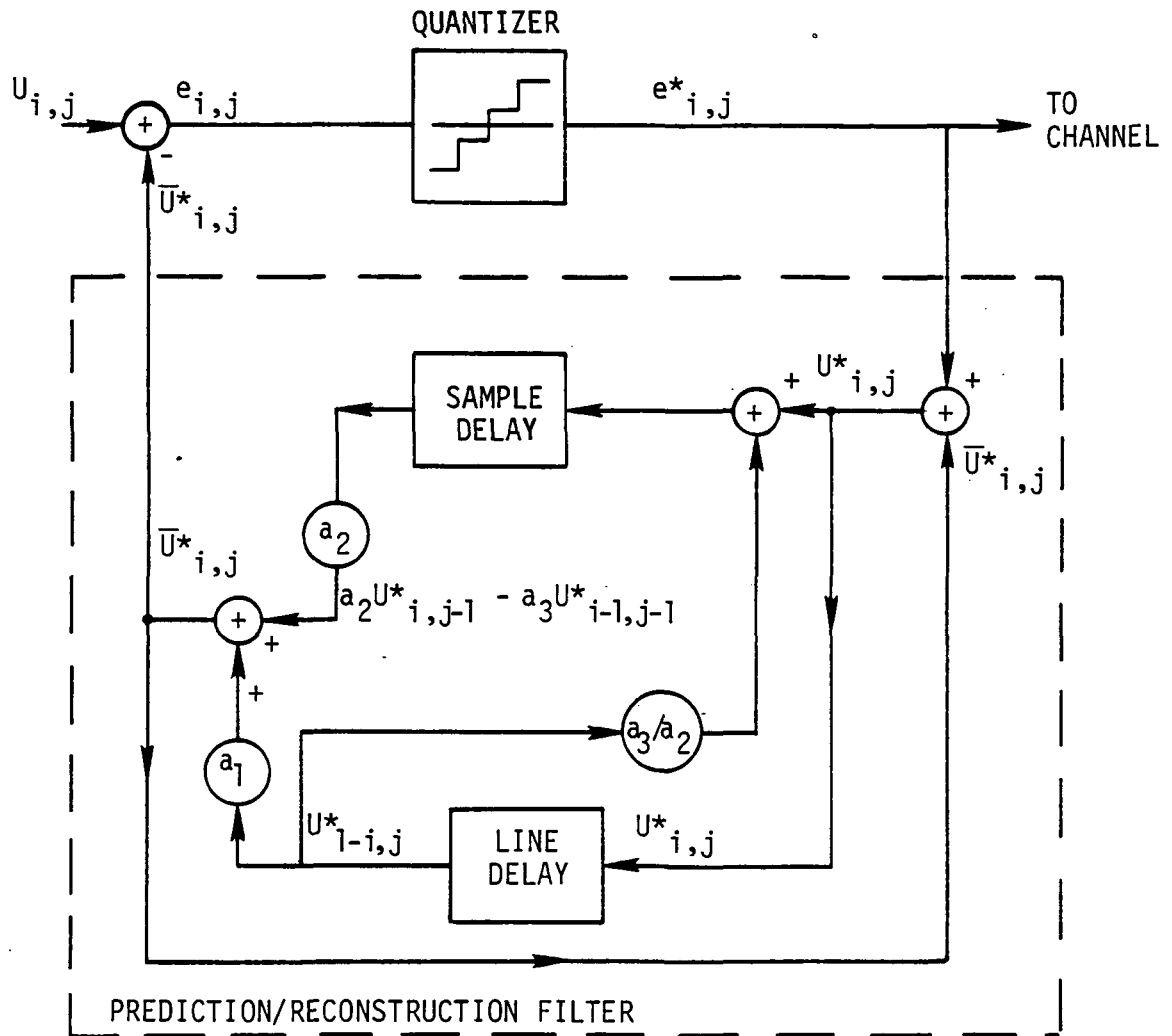


Figure 4-3. Two-dimensional DPCM. [5]

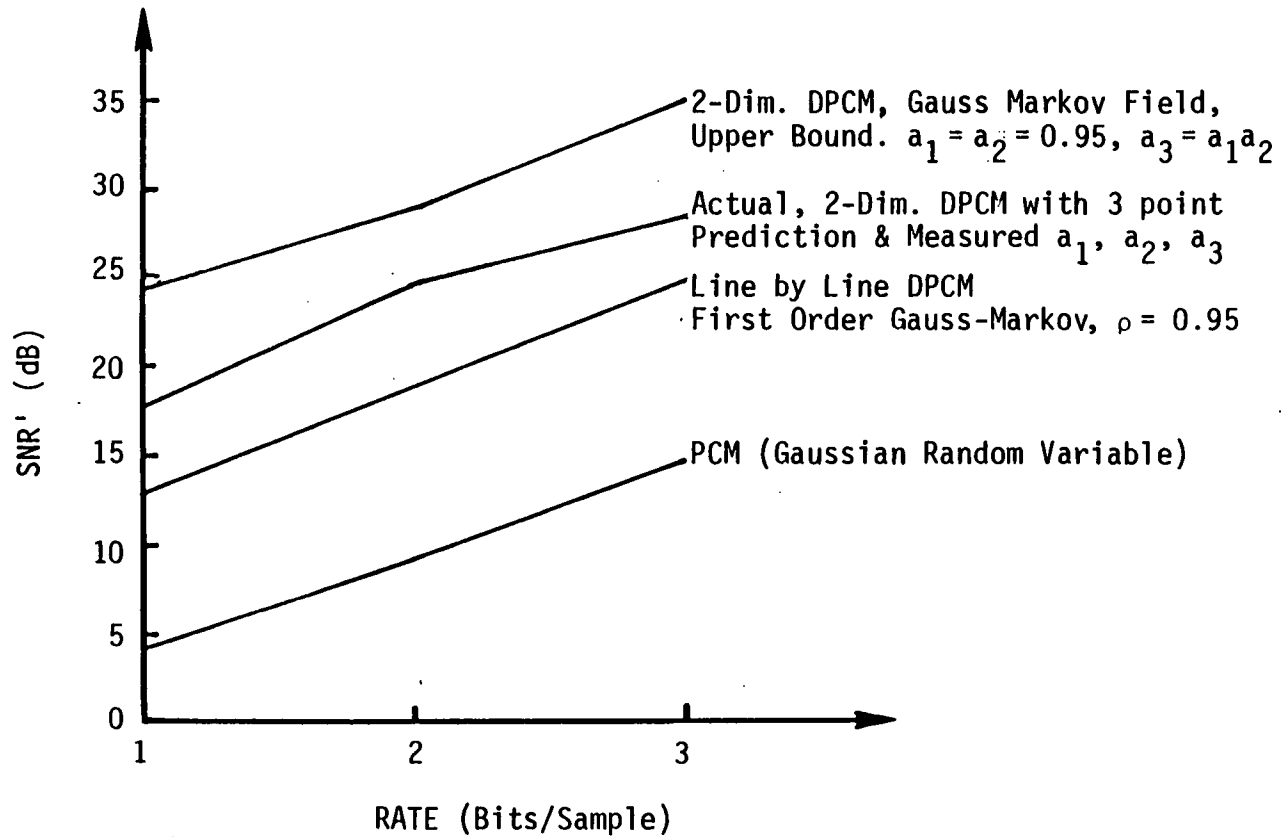


Figure 4-4. SNR versus rate of DPCM of two-dimensional, separable covariance causal model images and its comparison with line-by-line DPCM and with PCM. [5]

Figure 4-4 shows the performance of several DPCM methods and PCM. Typical compression ratios for two dimensional DPCM range (for typical 8-bit pixel images) from about 3 to 3.5.

DPCM is a simple easy to implement, on-line compression technique which can achieve useful compression ratios. Its three major drawbacks are:

- (1) its sensitivity to variation in image statistics,
- (2) its high sensitivity to channel errors, and
- (3) its increase in complexity for other types of data such as represented by autoregressive moving average models as opposed to autoregressive models only.

DPCM techniques can be adapted to local variations in image statistics by adjusting the number of quantization levels according to local scene activity and/or modifying the predictor rule whenever atypical features such as steep slopes or edges are encountered.

#### 4.6 DPCM With Multispectral Predictor

The previous discussion has indicated how the redundancy in an image, both temporally and spatially can be used to effectively realize data compression. In the case of multispectral imagery, yet another dimension exists which may provide further compression. This dimension is that of frequency. What is envisioned is to use the pixel value from one spectral band in the role of the predictor for subsequent bands. In this scheme, instead of the decoder being the replica of the encoder based on some model, the reference band would be transmitted intact using normal PCM and used at the receiver for reconstruction of the effected bands. Figure 4-5 indicates one possible realization of this idea. Notice that the predictor error has been eliminated and that, dependent upon the multiplex scheme adopted, the strong dependence on channel errors is likely reduced (i.e., channel errors affect the reference and the residuals in a like manner resulting in error cancellation for many cases).

As shown in Figure 4-5, each band is DPCM encoded by band (i.e., with respect to spatial redundancy) prior to spectral domain processing. Based on how the redundancy manifests itself this may not be the desired approach. Exactly how to implement this interactive encoding strategy should be the subject of further study.



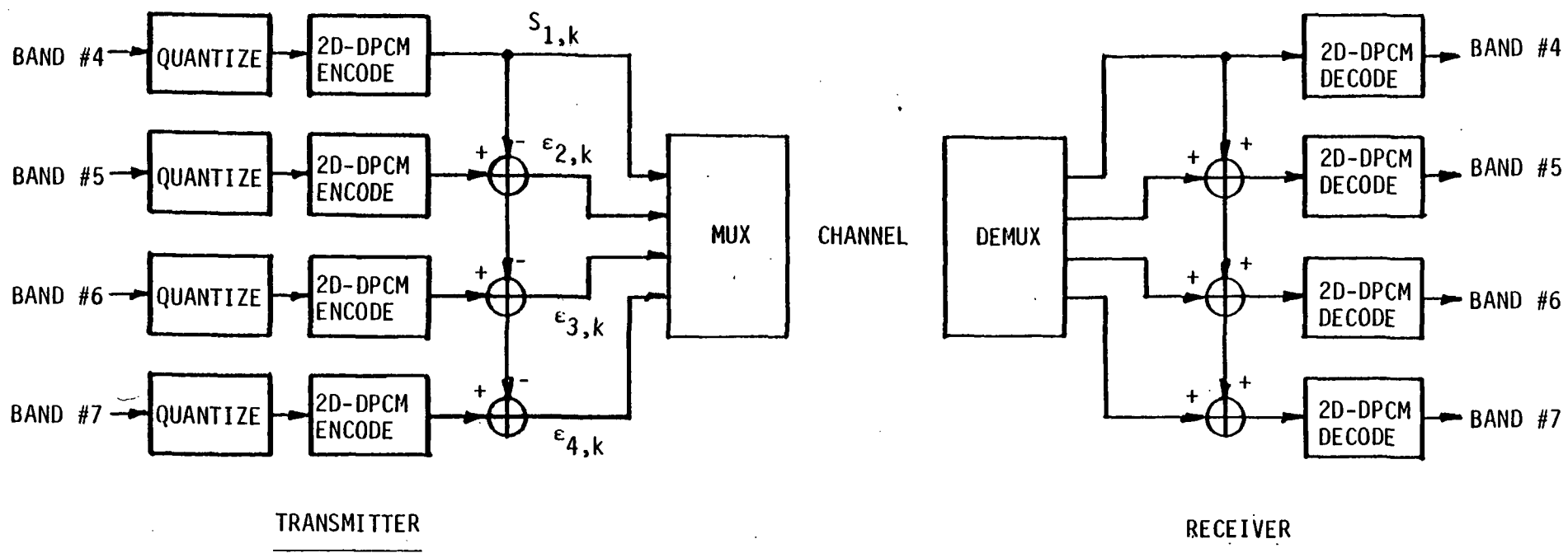


Figure 4-5. DPCM for multispectral data.

## 5.0 DYNAMIC COMPANDING

Histogram analyses of imagery as obtained with Landsat-type multispectral sensors routinely show that for a given frame, the full dynamic range of pixel amplitude available is seldom required. The histograms are generally narrow but with shifting mean value such that a wide range of probable values is required to accommodate the set of frames obtained as the satellite progresses in orbit.

Figure 5-1 shows a Landsat image of the North Carolina coastal area. Two areas, as defined by the rectangles, have been selected as candidates for histogram analysis to demonstrate the above point. The first area is inland and represents rural areas including sparse population (and is shown enlarged in Figure 5-2). The second provides a good land/water contrast comparison (and is shown enlarged in Figure 5-7). Figures 5-3 through 5-6 and 5-8 through 5-11 show histograms for the first and second areas, respectively. Each numbered bin on the histogram represents 2 counts in a 256 level gray scale. The data, however, only has a possible range of 128 gray levels (7-bit representation). Notice that for these areas the histograms are all generally contained in the first fifty or sixty gray levels with several being even narrower. This implies that a compression of 2-3 is possible if the data are encoded, say with a 5-6-bit representation.

Thus, variable length encoding with the code length and histogram position in the 7-bit code inserted into probably the secondary header would provide further compression over that achieved with band-to-band DPCM as described in the previous section.

It should be noted that exactly how band-to-band DPCM and dynamic companding should and even can work together is not at all clear. The approaches have been described independent of one another and no detailed examination of interaction has been addressed. This, as described in Section 7.0 is an area which should be addressed with further study.



Figure 5-1. MSS (band 6) from Landsat 2/North Carolina coastal waters (areas of analysis are shown in rectangular areas).

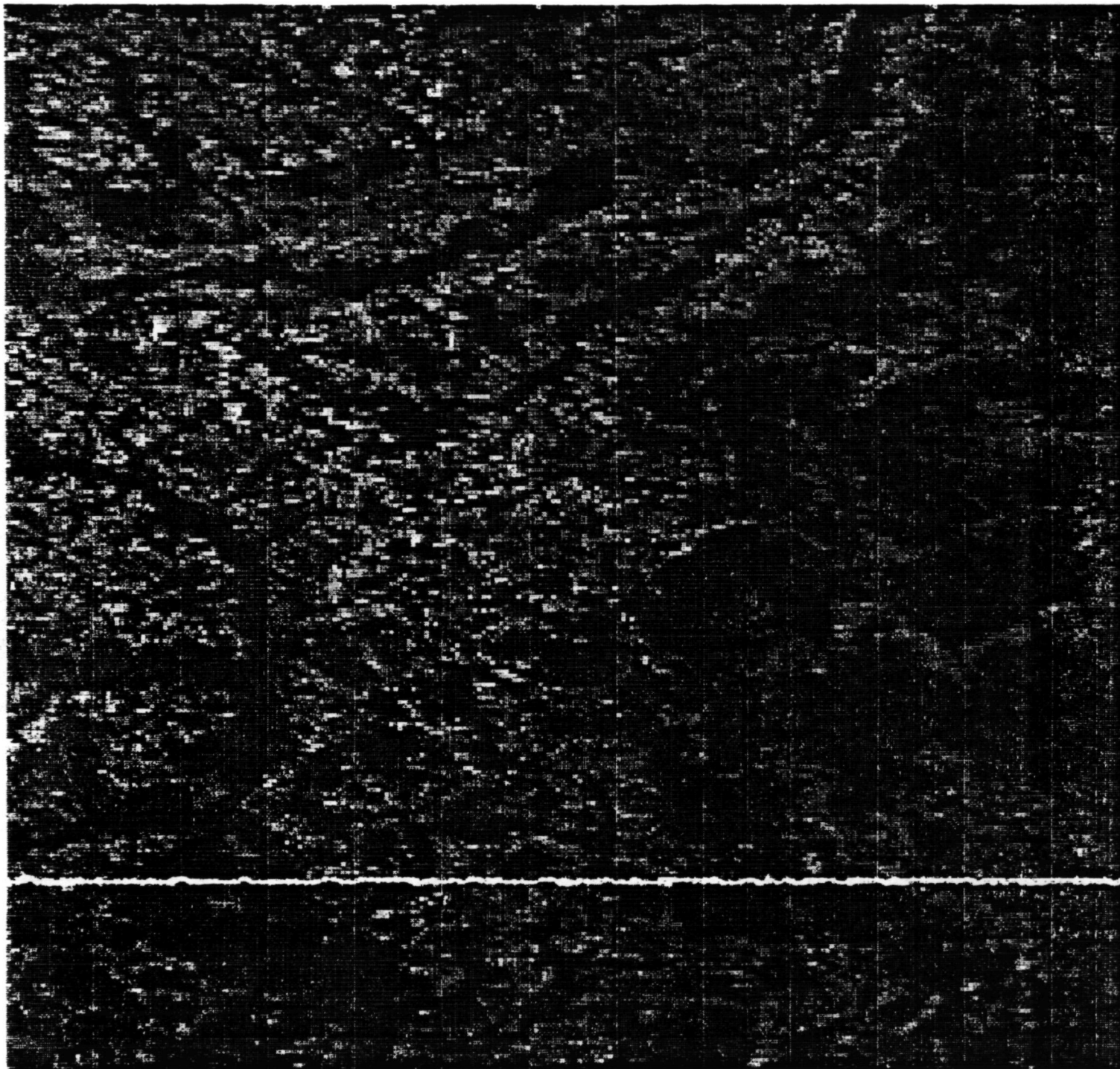
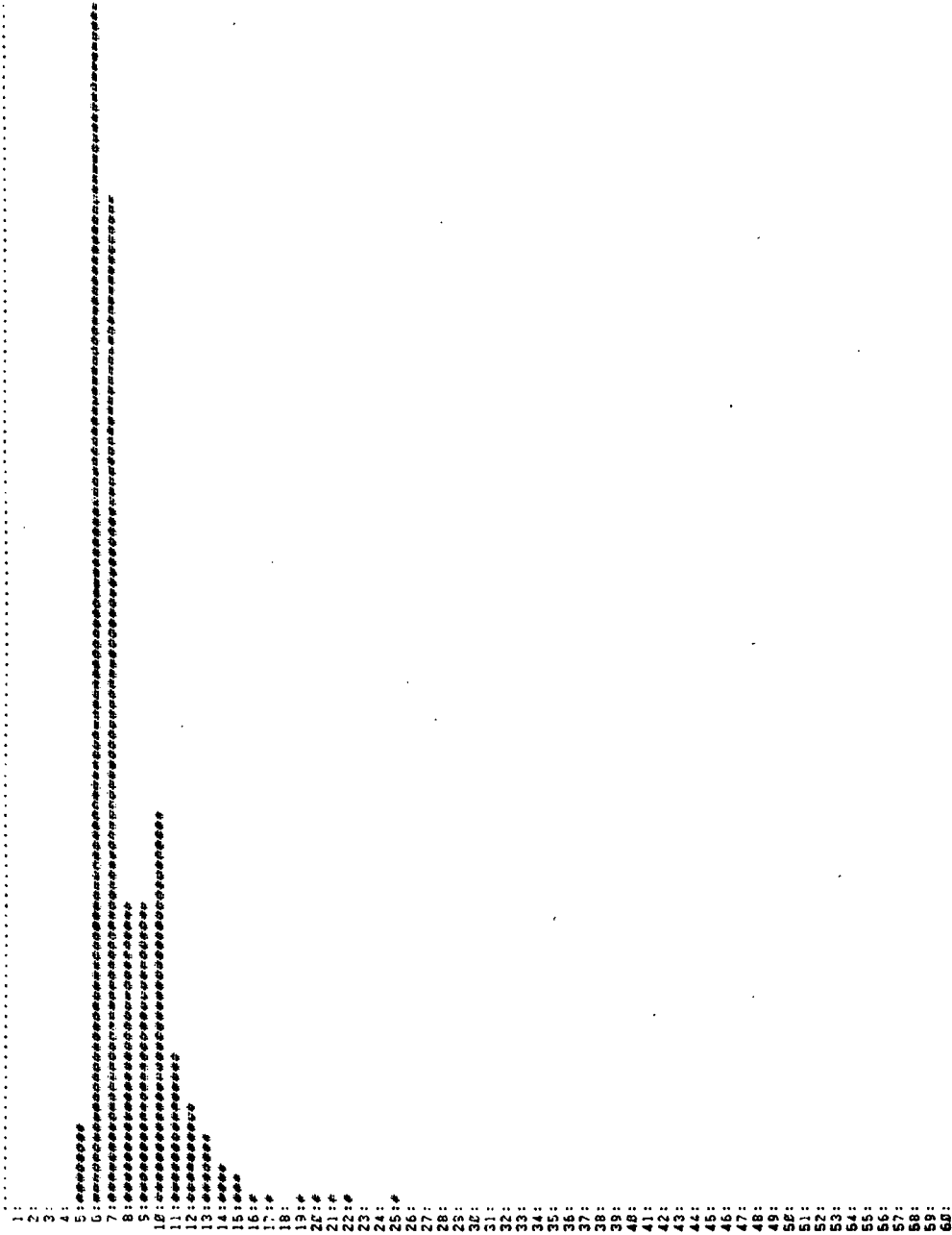


Figure 5-2. Analysis area no. 1, rural terrain.

GREY-LEVEL HISTOGRAM OF SIB1.IMG S1MSIZE= 2; LASTBINSIZE= 2  
 MAX1NUM=20998.0; MINIMUM= \*.0; THRESHOLD= +.17074111E+39



61:  
 62:  
 63:  
 64:  
 65:  
 66:  
 67:  
 68:  
 69:  
 70:  
 71:  
 72:  
 73:  
 74:  
 75:  
 76:  
 77:  
 78:  
 79:  
 80:  
 81:  
 82:  
 83:  
 84:  
 85:  
 86:  
 87:  
 88:  
 89:  
 90:  
 91:  
 92:  
 93:  
 94:  
 95:  
 96:  
 97:  
 98:  
 99:  
 100:  
 101:  
 102:  
 103:  
 104:  
 105:  
 106:  
 107:  
 108:  
 109:  
 110:  
 111:  
 112:  
 113:  
 114:  
 115:  
 116:  
 117:  
 118:  
 119:  
 120:

Figure 5-3. Histogram of first analysis area, band 4.

GREY-LEVEL HISTOGRAM OF S1B2.IMG      EINSIZE= 2: LASTBINSIZE= 2  
 MAXIMUM=14816.2: MINIMUM=      +.0: THRESHOLD= \*.1701411E+39



Figure 5-4. Histogram of first analysis area, band 5.

GREY-LEVEL HISTOGRAM OF 5183.IMG      BINSIZE= 2: LASTBINSIZE= 2  
 MAXIMUM=15676.8: MINIMUM=      +.8: THRESHOLD= +.1701411E+39



Figure 5-5. Histogram of first analysis area, band 6.

GREY-LEVEL HISTOGRAM OF SIB4.IMG    BINSIZE= 2; LASTBINSIZE= 2  
MAXIMUM=31783.0; MINIMUM=    .0; THRESHOLD= +.1701411E+39

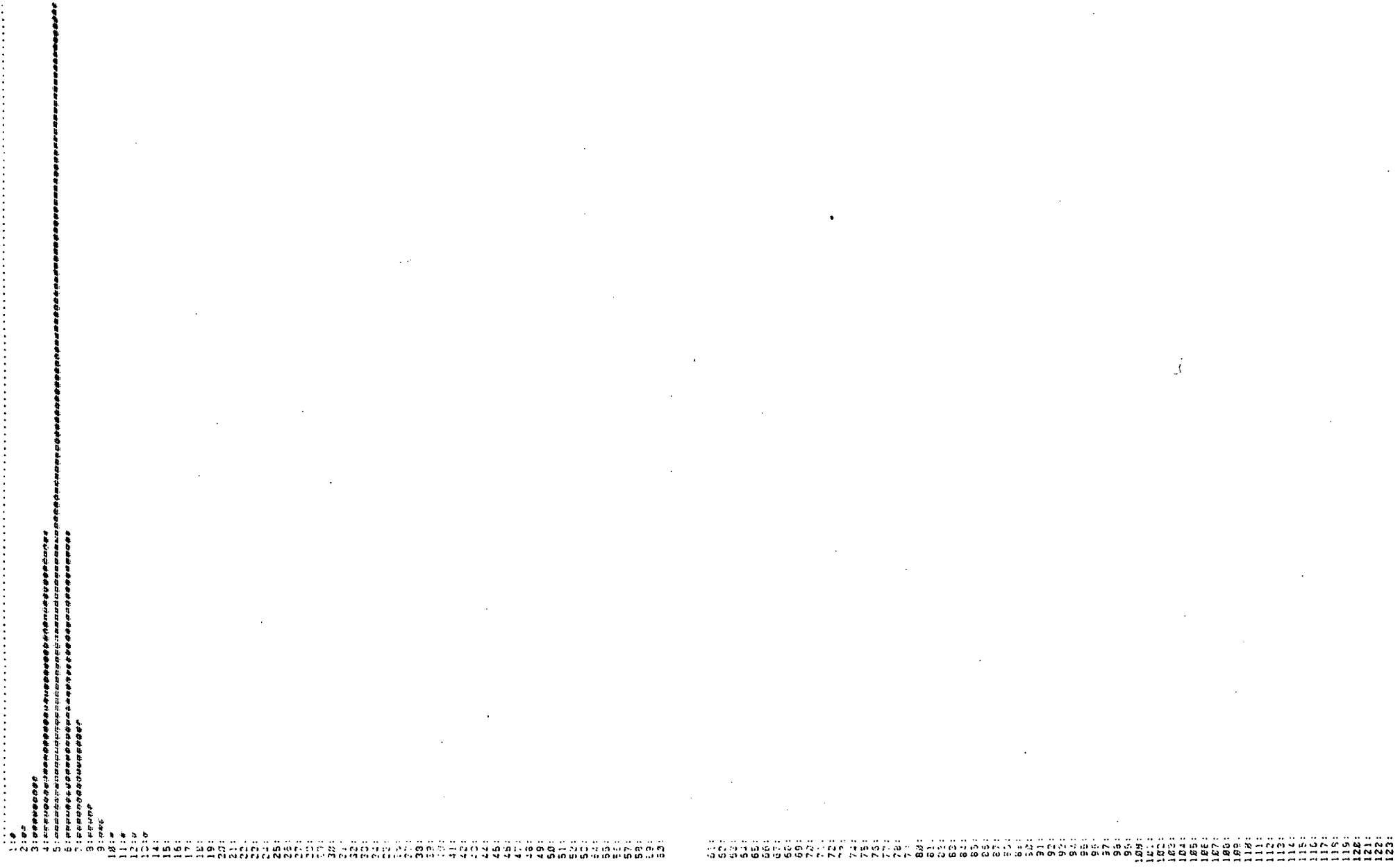


Figure 5-6. Histogram of first analysis area, band 7.





Figure 5-7. Analysis area no. 2, land/water contrast.

GREY-LEVEL HISTOGRAM OF 53B1.IMG  
MAXIMUM=31583.5; MINIMUM=

BINSIZE= 2; LASTBINSIZE= 2  
THRESHOLD= +.1781411E+39



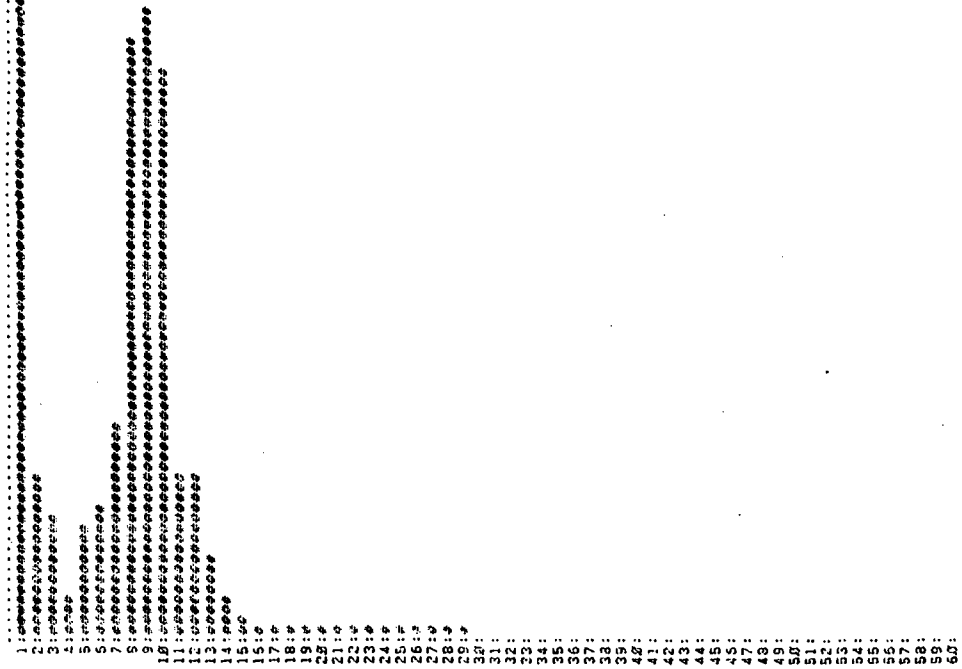
Figure 5-8. Histogram of analysis area no. 2, band 4.

GREY-LEVEL HISTOGRAM OF S3B2.IMG BINSIZE= 2: LASTBINSIZE= 2  
 MAXIMUM=2272.8: MINIMUM= 0.0: THRESHOLD= 1704111E+39



Figure 5-9. Histogram of analysis area no. 2, band 5.

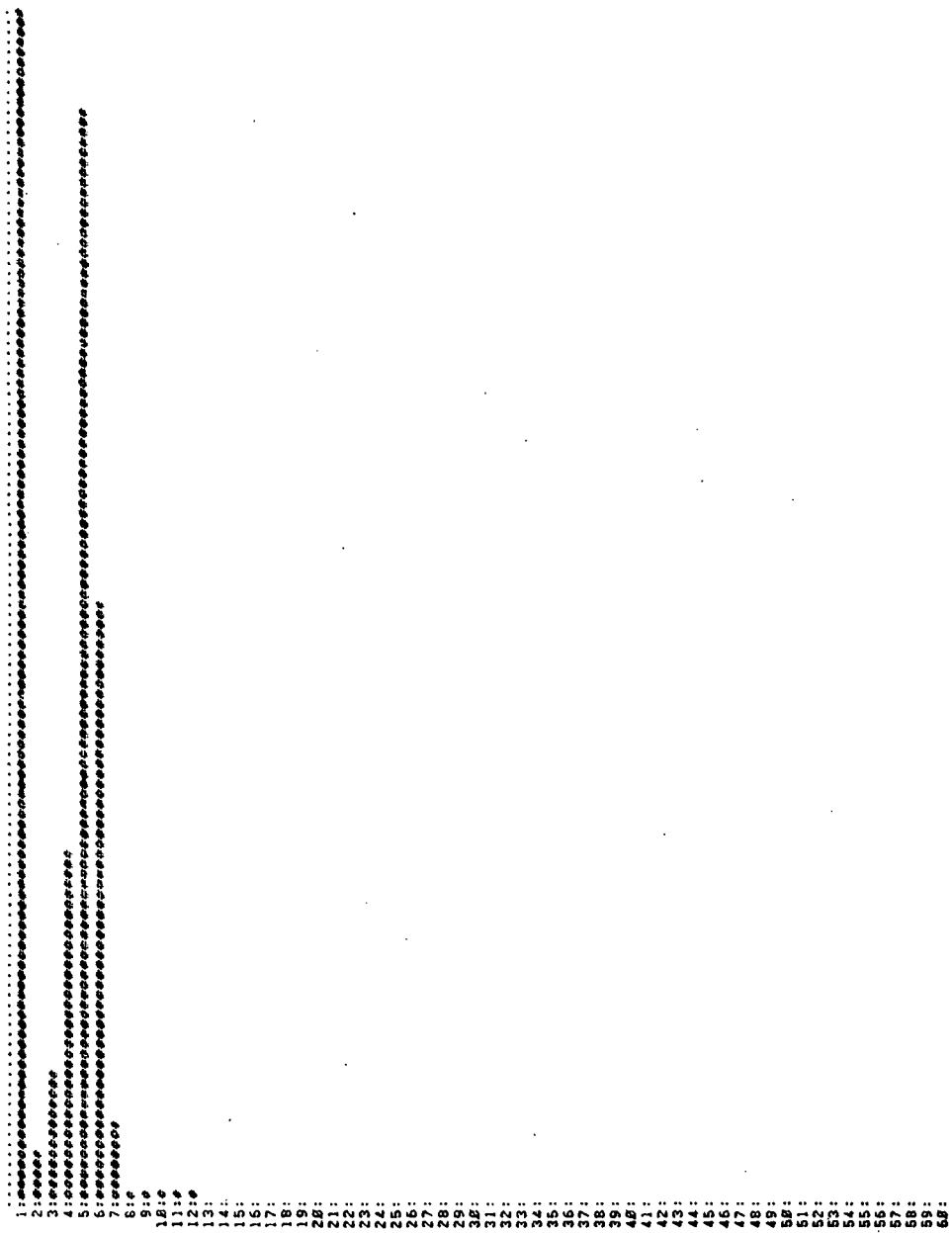
GREY-LEVEL HISTOGRAM OF S383.IMG BINSIZE= 2; LASTBINSIZE= 2  
 MAXIMUM=18317.0; MINIMUM=.....; THRESHOLD= +.17E+11IE+39



61:.....  
 62:.....  
 63:.....  
 64:.....  
 65:.....  
 66:.....  
 67:.....  
 68:.....  
 69:.....  
 70:.....  
 71:.....  
 72:.....  
 73:.....  
 74:.....  
 75:.....  
 76:.....  
 77:.....  
 78:.....  
 79:.....  
 80:.....  
 81:.....  
 82:.....  
 83:.....  
 84:.....  
 85:.....  
 86:.....  
 87:.....  
 88:.....  
 89:.....  
 90:.....  
 91:.....  
 92:.....  
 93:.....  
 94:.....  
 95:.....  
 96:.....  
 97:.....  
 98:.....  
 99:.....  
 100:.....  
 101:.....  
 102:.....  
 103:.....  
 104:.....  
 105:.....  
 106:.....  
 107:.....  
 108:.....  
 109:.....  
 110:.....  
 111:.....  
 112:.....  
 113:.....  
 114:.....  
 115:.....  
 116:.....  
 117:.....  
 118:.....  
 119:.....  
 120:.....  
 121:.....  
 122:.....  
 123:.....

Figure 5-10. Histogram of analysis area no. 2, band 6.

GREY-LEVEL HISTOGRAM OF S984.IMG  
 BIN SIZE= 2; LAST BIN SIZE= 2  
 MAXIMUM= 22149.5; MINIMUM= .....  
 THRESHOLD= +.1751411E+39



61:  
 62:  
 63:  
 64:  
 65:  
 66:  
 67:  
 68:  
 69:  
 70:  
 71:  
 72:  
 73:  
 74:  
 75:  
 76:  
 77:  
 78:  
 79:  
 80:  
 81:  
 82:  
 83:  
 84:  
 85:  
 86:  
 87:  
 88:  
 89:  
 90:  
 91:  
 92:  
 93:  
 94:  
 95:  
 96:  
 97:  
 98:  
 99:  
 100:  
 101:  
 102:  
 103:  
 104:  
 105:  
 106:  
 107:  
 108:  
 109:  
 110:  
 111:  
 112:  
 113:  
 114:  
 115:  
 116:  
 117:  
 118:  
 119:  
 120:  
 121:  
 122:  
 123:  
 124:

Figure 5-11. Histogram of analysis area no. 2, band 7.

## 6.0 ADDITIONAL TECHNIQUES FOR DATA RATE REDUCTION

Other, less desirable means of effecting data rate reduction which are fairly obvious include swath-width reduction, along-track truncation, and pixel averaging. The implementation of any of these should be data dependent and therefore adaptive. Swath-width reduction and along-track truncation are simply extensions of the FILE algorithm to other scene constituents. Pixel averaging, and the degree of averaging, is clearly application driven. It is hoped that the use of any of these can be avoided by use of DPCM and dynamic companding as described in the previous sections.

## 7.0 PACKETIZATION

The effect of data set selection on the packetization concept is minimal. Use of the FILE algorithm as well as dynamic companding force the need for some additional information to be located in the packet header: namely, the location of the deleted pixels in the case of FILE, and the location of max/min levels in the case of dynamic companding. FILE use strengthens any argument for variable length packets while dynamic companding produces a requirement for variable length words within the data packet itself.

## 8.0 RECOMMENDATIONS

In view of the preceeding discussion it is recommended that studies be conducted to:

- (1) Evaluate the potential performance of band-to-band DPCM by direct simulation. This would establish whether a temporal-spatial-spectral approach is feasible and would provide the tool to synthesize the specific technique.
- (2) Evaluate the potential performance improvement available with dynamic companding. This again can be achieved with simple simulation and the accumulation of imagery gray scale statistics.
- (3) Outline an overall adaptive strategy for utilizing the various compression techniques discussed here both collectively and selectively to achieve greater data compression in a data-dependent environment.
- (4) Assess the hardware requirements, power consumption, and throughput rates in implementing items (1), (2), and (3) with state-of-the-art technology such as VHSIC/VLSI.



## REFERENCES

1. Wilson, R. G. and W. E. Siverton, Jr., "Earth Feature Identification and Tracking Technology Development," presented at SPIE Engineers Technical Symposium East '79--Seminar on Smart Sensors in Washington, DC, April 17-20, 1979 (paper no. 178-14).
2. Greaves, J. R. and P. E. Sherr, "The Use of Cloud-Amount and Cloud-Type Statistics in the Design and Operation of Aerospace Systems," NTIS A70-30597, date unknown.
3. Sherr, Glaser, Barnes, and Willard, "World Wide Cloud Cover Distribution for Use in Computer Simulations," NASA CR 61226, June 1968.
4. Netravali, A. N. and J. O. Limb, "Picture Coding: A Review," Proc. IEEE, Vol. 8, No. 3, March 1980.
5. Jain, A. K., "Image Data Compression: A Review," Proc. IEEE, Vol. 69, No. 3, March 1981.

1. Report No. NASA CR 165970		2. Government Accession No.		3. Recipient's Catalog No.	
4. Title and Subtitle Concepts for On-Board Satellite Image Registration - Impact of Data Set Selection on Satellite On-Board Signal Processing				5. Report Date September 1982	
				6. Performing Organization Code	
7. Author(s) W. H. Ruedger, J. V. Aanstoos, W. E. Snyder				8. Performing Organization Report No. RTI/1796/00-04F	
9. Performing Organization Name and Address Research Triangle Institute P.O. Box 12194 Research Triangle Park, NC 27709				10. Work Unit No.	
				11. Contract or Grant No. NAS1-15768	
12. Sponsoring Agency Name and Address National Aeronautics and Space Administration Langley Research Center Hampton, VA 23665				13. Type of Report and Period Covered Contractor Report Jan. 1981 to July 1982	
				14. Sponsoring Agency Code	
15. Supplementary Notes Langley Technical Monitor: Marvin E. Beatty, III Final Report					
16. Abstract The NASA NEEDS program goals present a requirement for on-board signal processing to achieve user-compatible, information-adaptive data acquisition. This volume addresses the impact of data set selection on data formatting required for efficient telemetering of the acquired satellite sensor data. More specifically, the FILE algorithm developed by Martin-Marietta provides a means for the determination of those pixels for which the earth's surface is obscured by clouds. Subsequent deletion of these pixels from the data stream effects an improvement in the achievable system throughput. It will be seen that based on the lack of statistical stationarity in cloud cover, spatial distribution periods exist where data acquisition rates exceed the throughput capacity. The study therefore addresses various approaches to data compression and truncation as applicable to this sensor mission.					
17. Key Words (Suggested by Author(s)) On-board signal processing Data set selection Data compression				18. Distribution Statement Unclassified-Unlimited	
19. Security Classif. (of this report) Unclassified	20. Security Classif. (of this page) Unclassified	21. No. of Pages 35	22. Price		